Electronic Supplementary Information for Dalton Transactions

Dalton Transactions

Electronic Supplementary Information (ESI)

Triazolopyridines as ligands: structural diversity in iron(II), cobalt(II), nickel(II) and copper(II) complexes of 3-(2-pyridyl)-[1,2,4]triazolo[4,3-*a*]pyridine (L^{10}) and spin crossover in $[Fe^{II}(L^{10})_2(NCS)_2]$

Julia Klingele,*[a] Dominik Kaase,[a] Jakob Hilgert,[a] Gunther Steinfeld,[a] Marco H. Klingele[a] and Jochen Lach[b]

[a] *Institut für Anorganische und Analytische Chemie, Albert-Ludwigs-Universität Freiburg, Albertstr. 21, D-79104 Freiburg, Germany; E-mail: julia.klingele@ac.uni-freiburg.de; Fax: +49-(0)761-203-6001.*

[b] *Institut für Anorganische Chemie, Universität Leipzig, Johannisallee 29, D-04103 Leipzig, Germany.*

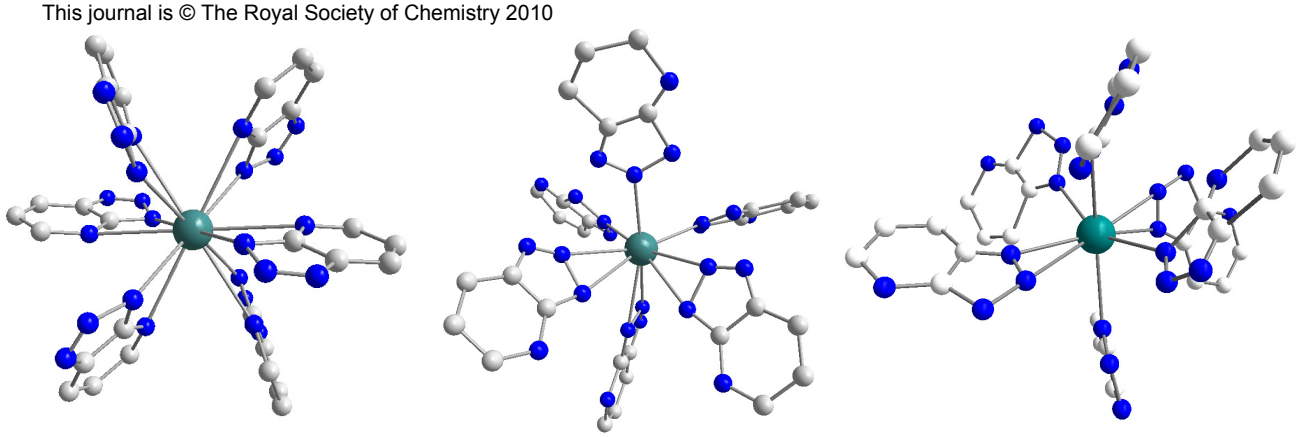

Fig. S1. Views of the three different coordination environments (N_{12}, N_9 and N_8) found in $[Eu^{II}(\mathbf{II})_2]$ (**1**). Hydrogen atoms have been omitted for clarity.

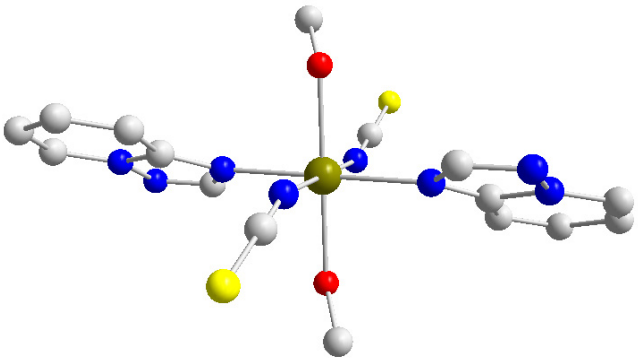

Fig. S2. View of the molecular structure of $[Fe^{II}(\mathbf{IV})_2(NCS)_2(MeOH)_2]$ (**2**). Hydrogen atoms have been omitted for clarity.

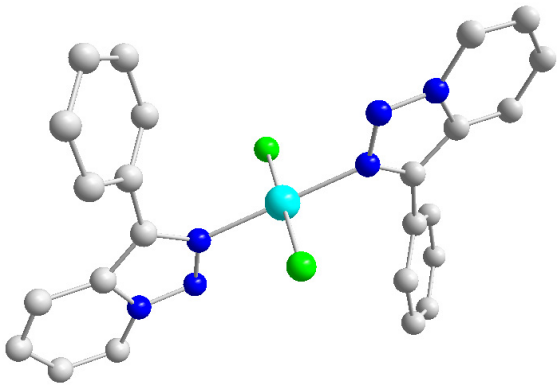

Fig. S3. View of the molecular structure of $[Cu^{II}(\mathbf{L^1})_2Cl_2]$ (**3**). Hydrogen atoms have been omitted for clarity.

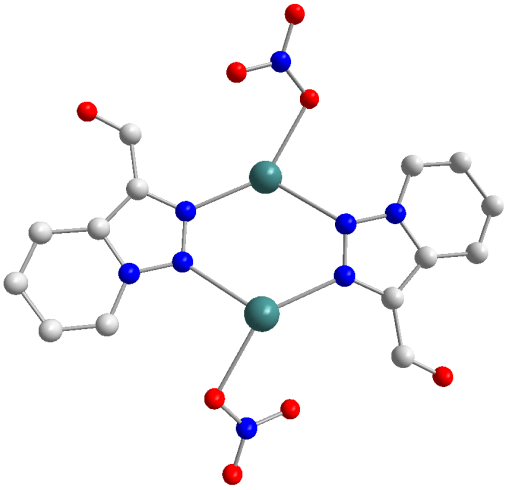

Fig. S4. View of the molecular structure of $[Ag^{I}_{2}(\mathbf{L}^{2})_{2}(NO_{3})_{2}]$ (**4**). Hydrogen atoms have been omitted for clarity.

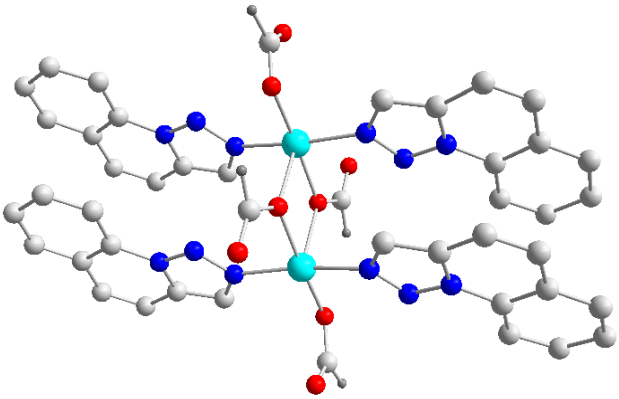

Fig. S5. View of the molecular structure of $[\{Cu^{II}(\mathbf{L}^{3})_{2}(HCO_{2})\}_{2}(\mu\text{-}HCO_{2})_{2}]\cdot 4H_{2}O$ (**5**). Hydrogen atoms, except those of the HCO_{2}^{-} co-ligands, and solvate molecules have been omitted for clarity.

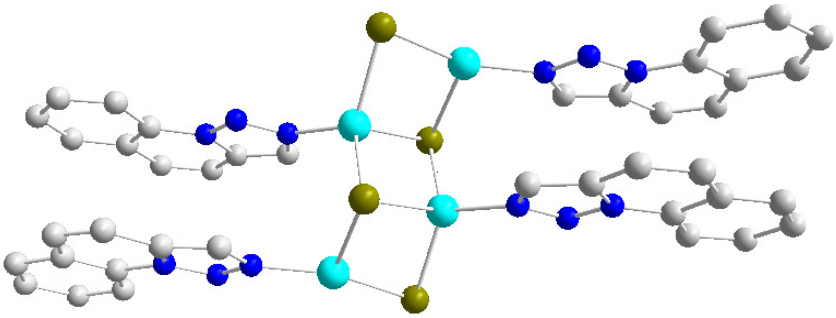

Fig. S6. View of the molecular structure of $[Cu^{I}_{4}(\mathbf{L}^{3})_{4}(\mu\text{-}Br)_{2}(\mu_{3}\text{-}Br)_{2}]$ (**6**). Hydrogen atoms have been omitted for clarity.

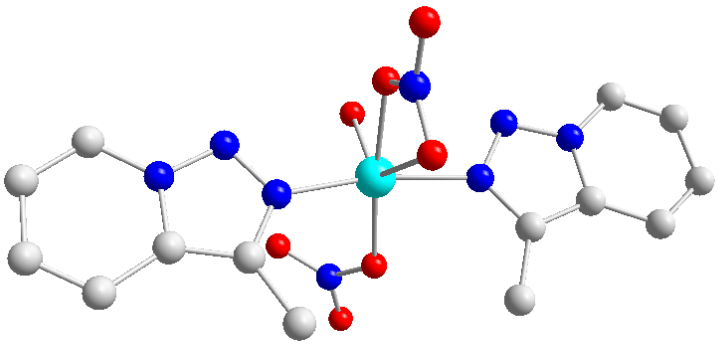

Fig. S7. View of the molecular structure of $[Cu^{II}(\mathbf{L}^{4})_2(NO_3)_2(H_2O)]$ (**7**). Hydrogen atoms have been omitted for clarity.

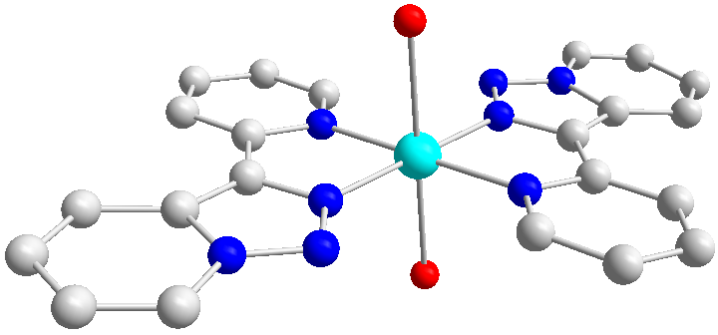

Fig. S8. View of the molecular structure of the complex cation of $[Cu^{II}(\mathbf{L}^{5})_2(H_2O)_2](NO_3)_2$ (**8**). Hydrogen atoms have been omitted for clarity.

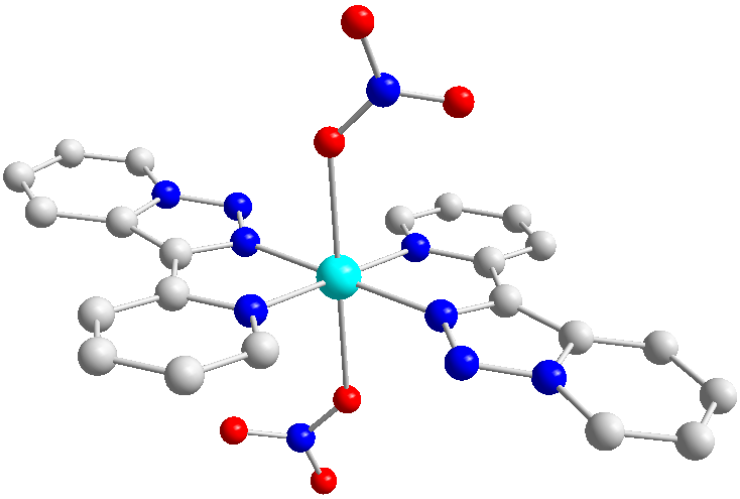

Fig. S9. View of the molecular structure of $[Cu^{II}(\mathbf{L}^{5})_2(NO_3)_2]$ (**9**). Hydrogen atoms have been omitted for clarity.

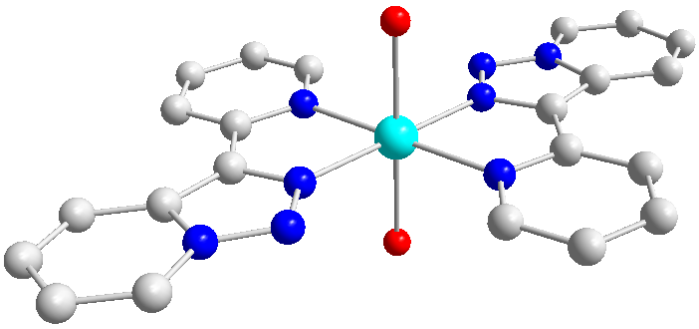

Fig. S10. View of the molecular structure of the complex cation of $[Cu^{II}(\mathbf{L}^5)_2(H_2O)_2](ClO_4)_2$ (**10**). Hydrogen atoms have been omitted for clarity.

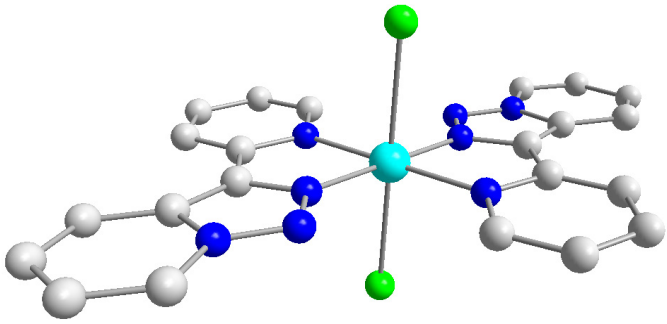

Fig. S11. View of the molecular structure of $[Cu^{II}(\mathbf{L}^5)_2Cl_2]\cdot MeOH\cdot 2H_2O\cdot HCl$ (**11**). Hydrogen atoms and solvate molecules have been omitted for clarity.

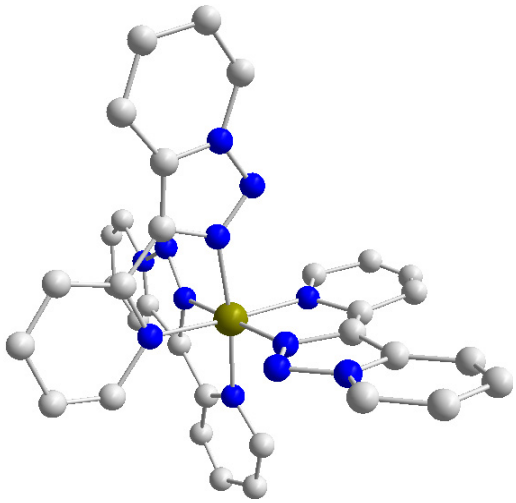

Fig. S12. View of the molecular structure of the complex cation of $[Fe^{II}(\mathbf{L}^5)_3](BF_4)_2$ (**12**). Hydrogen atoms have been omitted for clarity.

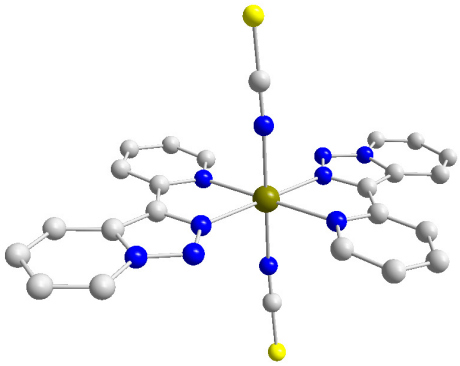

Fig. S13. View of the molecular structure of $[Fe^{II}(\mathbf{L^5})_2(NCS)_2]\cdot 2CHCl_3$ (**13**). Hydrogen atoms and solvate molecules have been omitted for clarity.

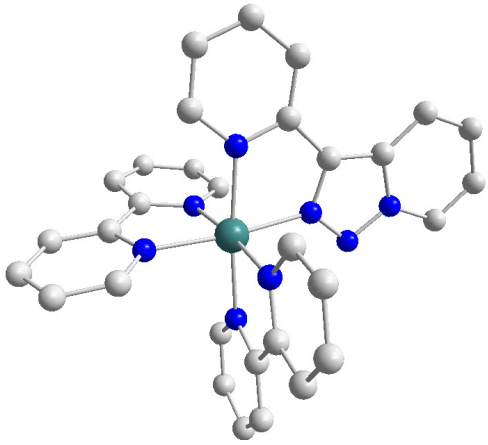

Fig. S14. View of the molecular structure of the complex cation of $[Ru^{II}(\mathbf{L^5})(bpy)_2](PF_6)_2$ (**14**). Hydrogen atoms have been omitted for clarity.

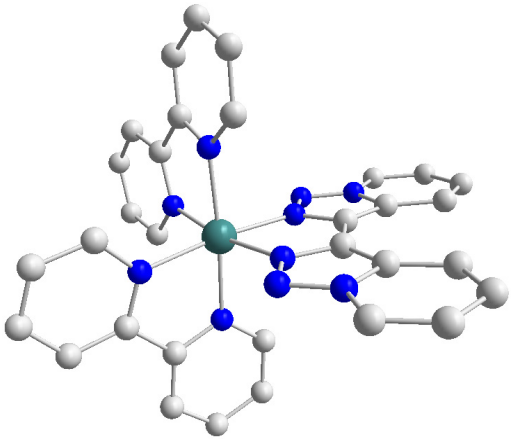

Fig. S15. View of the molecular structure of the complex cation of $[Ru^{II}(\mathbf{L^6})(bpy)_2](PF_6)_2$ (**15**). Hydrogen atoms have been omitted for clarity.

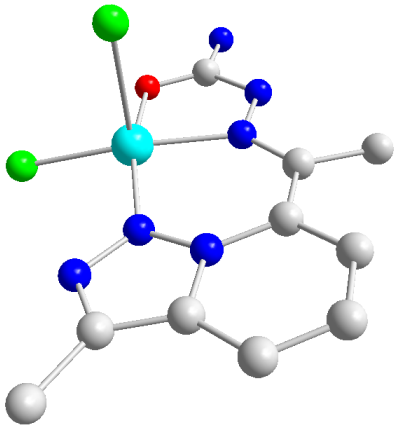

Fig. S16. View of the molecular structure of $[Cu^{II}(\mathbf{L}^{7})Cl_2]\cdot 2.5H_2O$ (**16**). Hydrogen atoms and solvate molecules have been omitted for clarity.

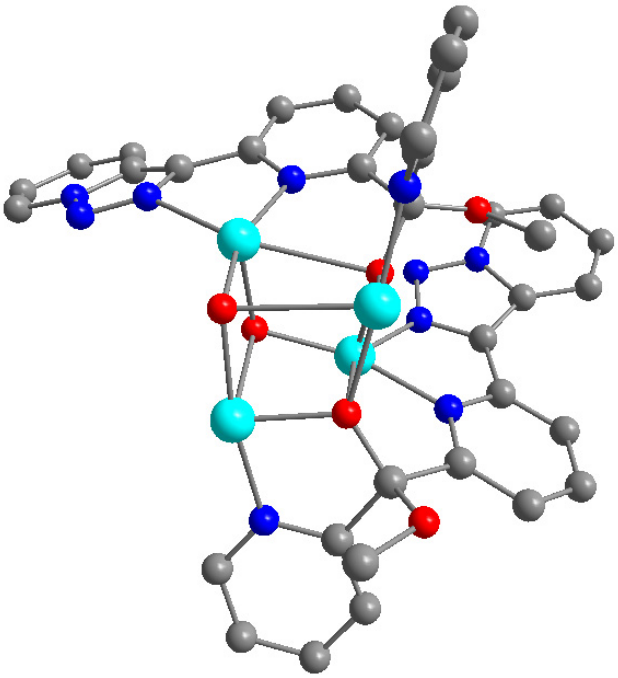

Fig. S17. View of the molecular structure of the complex cation of $[\{Cu^{II}(\mathbf{L}^{8})\}_4](NO_3)_4\cdot 8H_2O$ (**17**). Only two of the four ligands $\mathbf{L}^{8}$ are shown. Hydrogen atoms have been omitted for clarity.

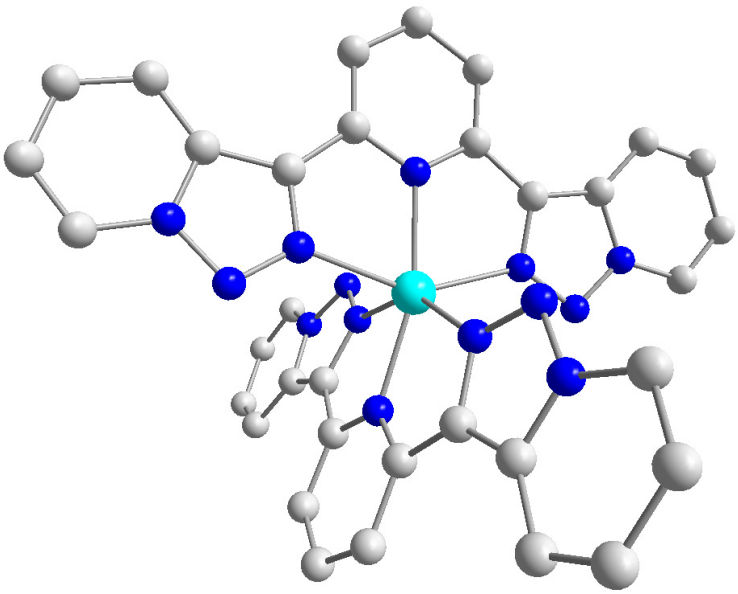

Fig. S18. View of the molecular structure of the complex cation of $[Zn^{II}(\mathbf{L}^{9})_2](ClO_4)_2 \cdot 0.5MeCN$ (**18**). Hydrogen atoms have been omitted for clarity.

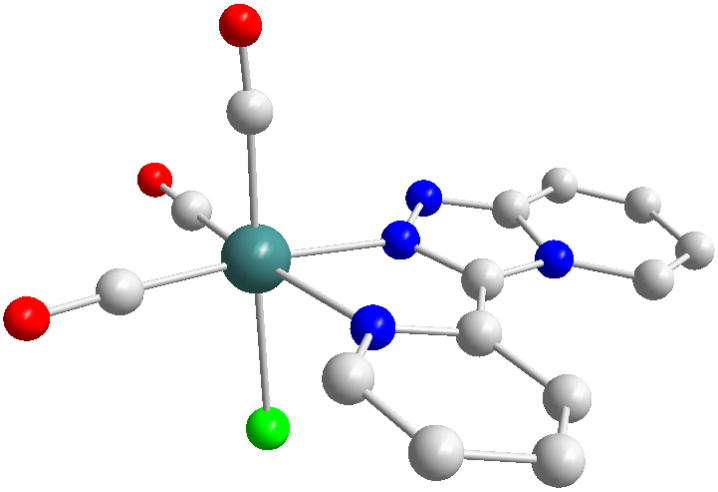

Fig. S19. View of the molecular structure of $[Re^{I}(\mathbf{L}^{10})(CO)_3Cl]$ (**19**). Hydrogen atoms have been omitted for clarity.

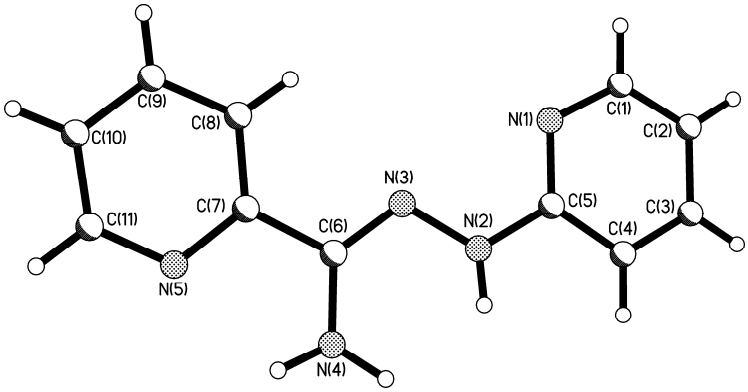

Fig. S20. View of the molecular structure of *N*-(2-pyridylamino)-2-pyridineamidine (**XV**).

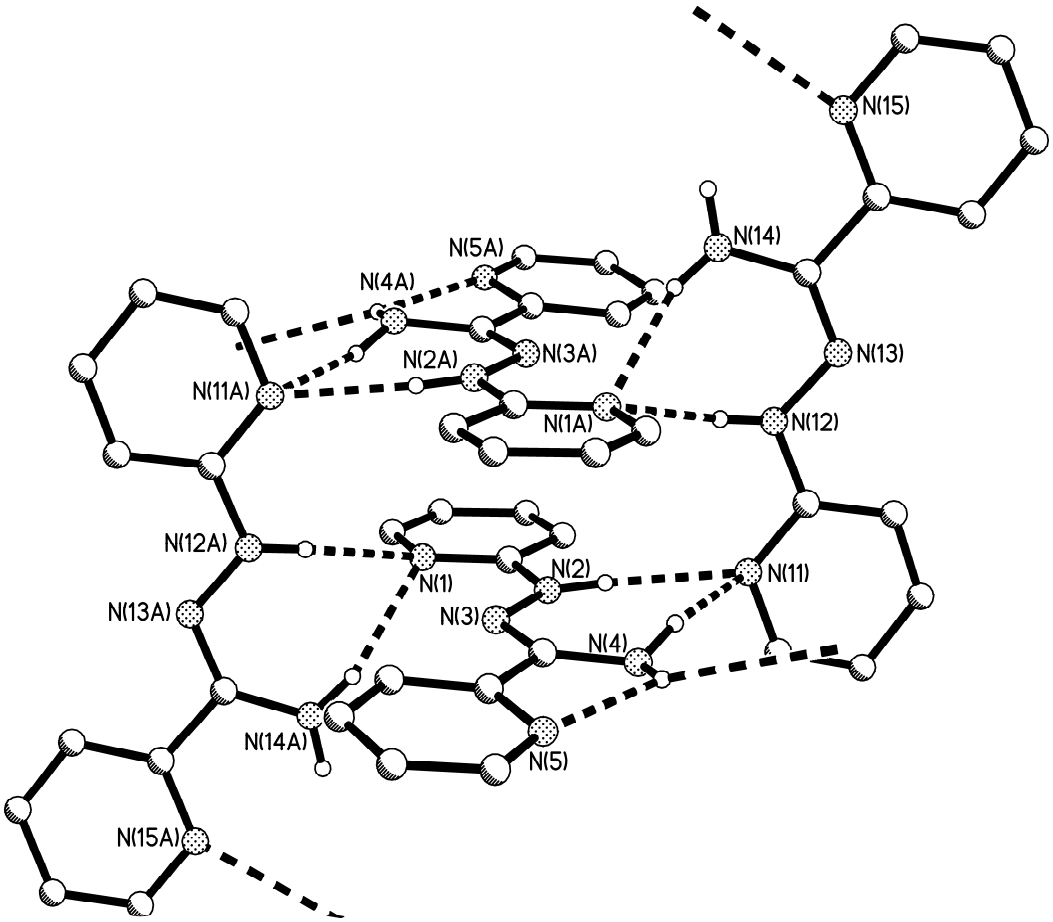

Fig. S21. Hydrogen bonding in the crystal structure of *N*-(2-pyridylamino)-2-pyridineamidine (**XV**). Selected distances [Å]: N(1)···H–N(12A) 3.007, N(1)···H–N(14A) 3.041, N(2)–H···N(11) 3.011, N(4)–H···N(11) 3.045, N(4)–H···N(5) 2.641, N(4)–H···N(15B) 3.350. Symmetry operations used to generate equivalent atoms: (A) –x+1, –y+1, –z; (B) x, –y+1.5, z+0.5.

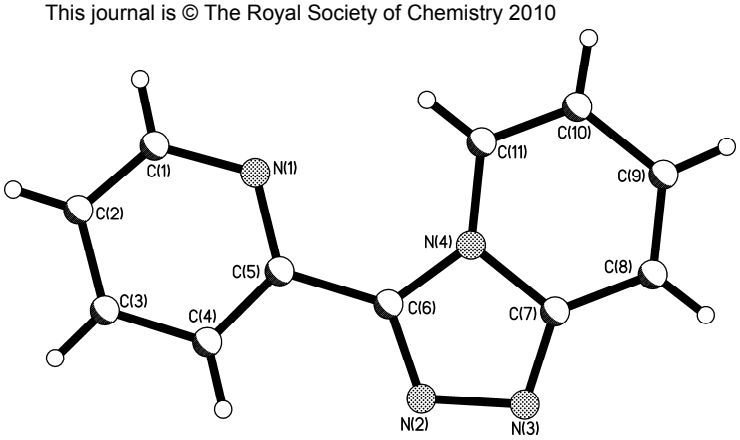

Fig. S22. View of the molecular structure of 3-(2-pyridyl)-[1,2,4]triazolo[4,3-*a*]pyridine (**L**[10]).

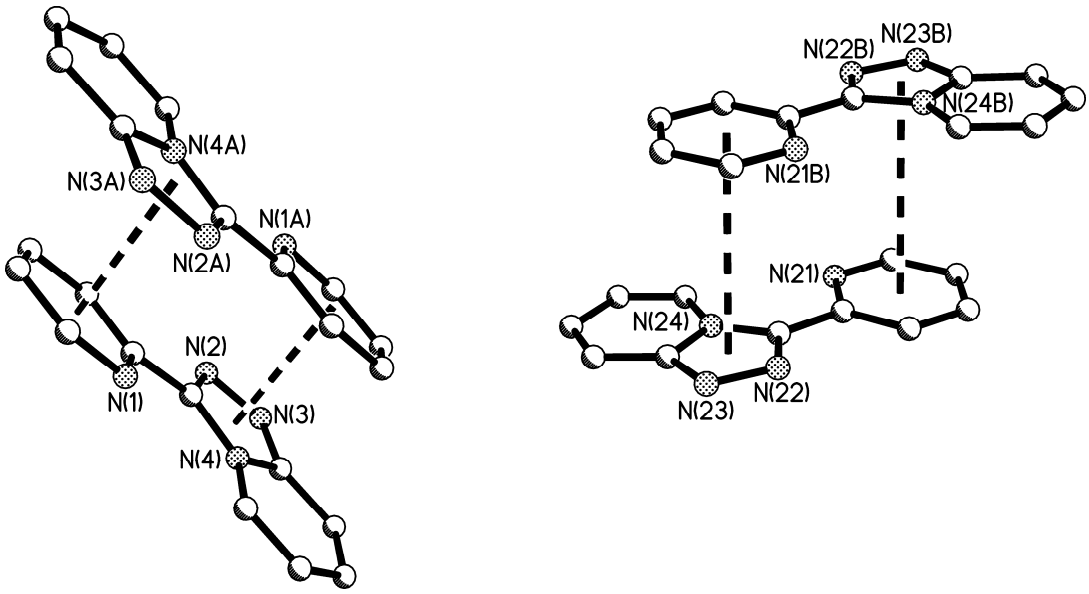

Fig. S23. π–π Stacking in the crystal structure of 3-(2-pyridyl)-[1,2,4]triazolo[4,3-*a*]pyridine (**L**[10]). Selected distances [Å]: cent<N(1)/C(1)/C(2)/C(3)/C(4)/C(5)>···cent<N(2A)/N(3A)/N(4A)/C(6A)/C(7A)> 3.387, cent<N(21)/C(21)/C(22)/C(23)/C(24)/C(25)>···cent<N(22B)/N(23B)/N(24B)/C(26B)/C(27B)> 3.712. Symmetry operations used to generate equivalent atoms: (A) –x +1, –y, –z+1; (B) –x+2, –y+2, –z.

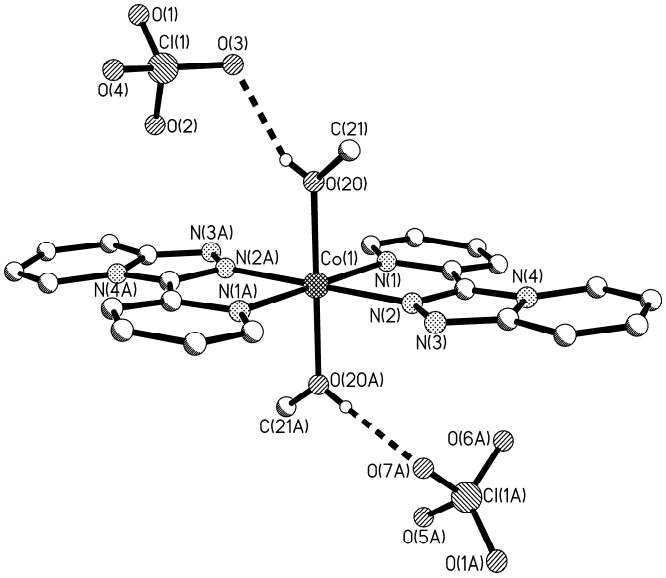

Fig. S24. View of the molecular structure of $[Co^{II}(\mathbf{L^{10}})_2(MeOH)_2](ClO_4)_2$ (**20**). Hydrogen atoms, except those of the hydroxyl groups of the MeOH co-ligands, have been omitted for clarity. The hydrogen-bonded ClO_4^- counterion is disordered over two positions with site occupancy factors of 0.50 [O(2)–O(4)] and 0.50 [O(5)–O(7)], twirling around the Cl(1)–O(11) bond. Selected distances [Å]: Co(1)–N(1) 2.139(2), Co(1)–N(2) 2.094(2), Co(1)–O(20) 2.093(2), O(3)···O(20) 2.740, O(7A)···O(20A) 2.806. Selected angles [°]: N(1)–Co(1)–N(2) 77.06(7), N(1)–Co(1)–O(20) 91.95(8), N(1)–Co(1)–N(2A) 102.94(7), N(1)–Co(1)–O(20A) 88.05(8), N(2)–Co(1)–O(20) 91.30(8), N(2)–Co(1)–O(20A) 88.70(8). Symmetry operation used to generate equivalent atoms: (A) –x, –y+2, –z.

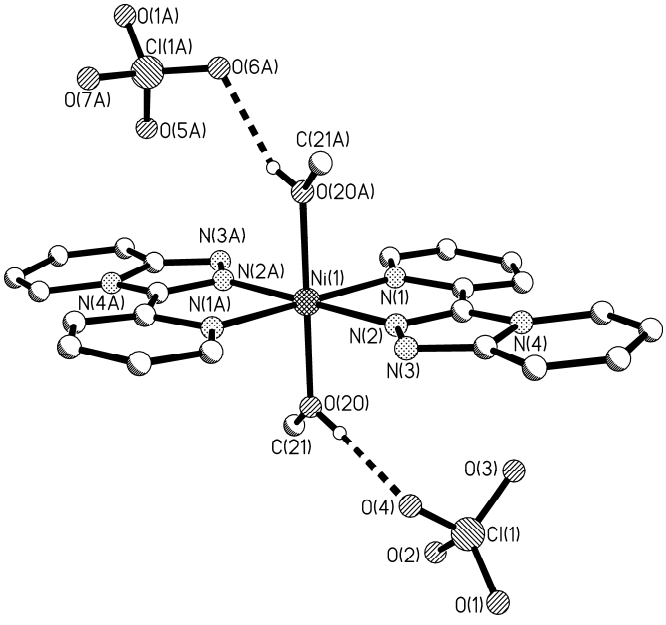

Fig. S25. View of the molecular structure of $[Ni^{II}(\mathbf{L^{10}})_2(MeOH)_2](ClO_4)_2$ (**21**). Hydrogen atoms, except those of the hydroxyl groups of the MeOH co-ligands, have been omitted for clarity. The hydrogen-bonded ClO_4^- counterion is disordered over two positions with site occupancy factors of 0.59 [O(2)–O(4)] and 0.41 [O(5)–O(7)], twirling around the Cl(1)–O(11) bond. Selected distances [Å]: Ni(1)–N(1) 2.108(2), Ni(1)–N(2) 2.070(2), Ni(1)–O(20) 2.052(2), O(4)···O(20) 2.857, O(6A)···O(20A) 2.747. Selected angles [°]: N(1)–Ni(1)–N(2) 79.28(8), N(1)–Ni(1)–O(20) 89.88(9), N(1)–Ni(1)–N(2A) 100.72(8), N(1)–Ni(1)–O(20A) 90.12(9), N(2)–Ni(1)–O(20) 88.81(9), N(2)–Ni(1)–O(20A) 91.19(9). Symmetry operation used to generate equivalent atoms: (A) –x, –y, –z.

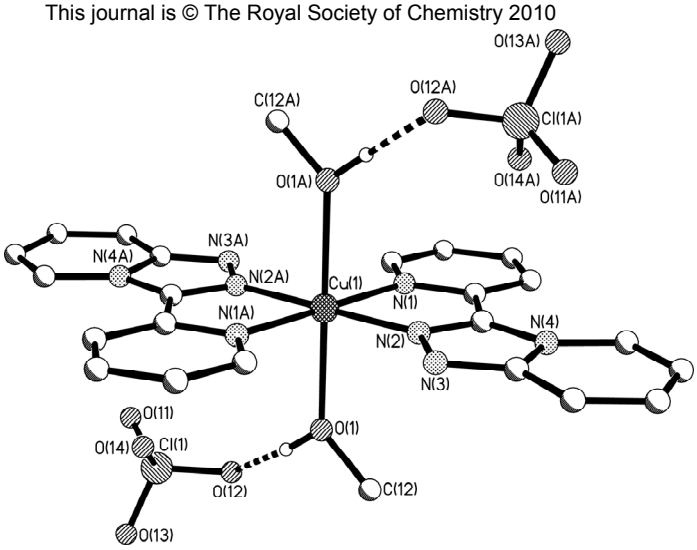

Fig. S26. View of the molecular structure of $[Cu^{II}(\mathbf{L^{10}})_2(MeOH)_2](ClO_4)_2$ (**22**). Hydrogen atoms, except those of the hydroxyl groups of the MeOH co-ligands, have been omitted for clarity. Selected distances [Å]: Cu(1)–N(1) 2.057(3), Cu(1)–N(2) 1.984(3), Cu(1)–O(1) 2.347(3), O(1)···O(12) 2.844. Selected angles [°]: N(1)–Cu(1)–N(2) 79.62(13), N(1)–Cu(1)–O(1) 90.45(12), N(1)–Cu(1)–N(2A) 100.38(13), N(1)–Cu(1)–O(1A) 89.55(12), N(2)–Cu(1)–O(1) 89.92(12), N(2)–Cu(1)–O(1A) 90.08(12). Symmetry operation used to generate equivalent atoms: (A) –x,